Influence of Polymer Characteristics and Melt-Spinning Conditions on the Production of Fine Denier Poly(Ethylene Terephtalate) Fibers. Part III. Structure and Properties of Fine Denier As-Spun PET Fibers

CHANG T. KIANG* and JOHN A. CUCULO†

North Carolina State University, Fiber and Polymer Science, Raleigh, North Carolina 27695-8302

SYNOPSIS

The effect of decreasing take-up denier on the structure and mechanical properties of as-spun poly(ethylene terephtalate) (PET) fibers is shown to be, in general, similar to an increase of take-up velocity. Both can be related to increased threadline cooling rate and increased spinline stress that control the structure development in the threadline. However, important distinctions were observed in the orientation and crystallization effects due to decrease of take-up denier or increase of take-up velocity. These distinctions were explained on the basis of the threadline dynamics study of the fine denier PET fiber in the high-speed spinning process, discussed in Part II of this study. Other properties, such as the dynamic mechanical properties and dye uptake, are not related to individual structure parameters, depending on the overall changes in structure, e.g., as given by the free volume.

INTRODUCTION

The growing interest on fine denier fibers, i.e., fibers with less than 1 denier per filament (dpf), can be linked to the special properties they impart on fabrics and apparel products. Besides the light weight and softness of the final product, an outstanding waterproofing-moisture permeable effect can be obtained due to the small spaces between fibers.[1] Filtration[2] and wiping cloths[3] are also major applications that benefit from the small pore sizes that can be achieved with these fibers. Additionally, yarn strength has been reported to increase with the decrease of the denier of the individual fibers.[4]

In this study we concentrate on the characterization of the structure and mechanical properties of the fine denier as-spun fibers obtained in high-speed spinning. The spinning conditions have been described in Part II of this series.[5] In analyzing the structure of these fibers, it is hoped to fill the scarcity of information extant in this area since Matsui's report on the crystallinity suppression with decrease of denier[6] as well as to compare the effect of decreasing denier with the better known effects of increasing spinning speeds.

EXPERIMENTAL

Materials

As-spun poly(ethylene terephtalate) (PET) fibers obtained in spinning speeds ranging from 2000 to 7000 m/min were employed. These fibers are produced from the low intrinsic viscosity (IV) PET polymers characterized in Part I,[7] namely polymer A (IV 0.56) and polymer B (IV 0.64). Unless otherwise noted, polymer A is employed throughout this study. Polymer B is included in those cases where we want to compare the effect of the fiber dpf at different take-up speeds. It was shown in the earlier papers[5,7] that these polymers showed distinct rheological and spinning behavior, which reflected in the minimum attainable as-spun fiber denier. However, it was also shown that the effect of the fiber dpf and

* Present address: Rhodia S.A., Sao Paulo, S.P., Brazil.
† To whom correspondence should be addressed.

Journal of Applied Polymer Science, Vol. 46, 83–97 (1992)
 CCC 0021-8995/92/010083-15$04.00

take-up speed on the threadline dynamics is much larger than the effect of the rheological property difference from polymers A and B. Therefore, it seems reasonable to assume that the structure characteristics are mainly determined by the spinning speed and the fiber denier, irrespective to the polymer A or B employed.

The fibers were melt spun in a Fourne extruder through a 14-hole spinneret, with capillary diameter of 0.23 mm and length to diameter ratio of 2.3, at the extrusion temperature of 295°C, as described in Part II.[5] The spinnability deteriorates at take-up speeds above 5000 m/min, especially for fiber denier below 1 dpf. In these cases a 4-cm-thick insulation plate is placed at the exit of the spinneret as well as a convergence guide, placed at 70 cm from the spinneret. More details are given in Part II.[5]

Birefringence

The mean birefringence was determined with the compensation method, as described in Part II.[5]

Differential Scanning Calorimeter (DSC)

The thermal analyses were performed on a Perkin-Elmer DSC-7 differential scanning calorimeter. The system comprises an intracooler and TAC7/7 instrument controller. Data analysis were executed on a PE 7700 professional computer and data were plotted on a Graphics Plotter 8. Approximately 10 mg of the fiber sample, knotted together, were used in each run. DSC curves were obtained in the first heating, in the temperature range of 25–300°C and with a heating rate of 10 K/min.

Density

Density was measured on small loops of the fiber sample with a density gradient column at 23°C, according to the ASTM method D1505-68. The column liquid used was an aqueous sodium bromide solution. In order to eliminate air bubbles and to improve the wettability, the samples were centrifuged in the solution prior to introduction into the column.

Volume fraction crystallinity K_d was obtained from the following relation:

$$K_d = \frac{\rho - \rho_a}{\rho_c - \rho_a} \tag{1}$$

where ρ is the measured fiber density, ρ_a and ρ_c are, respectively, the density of a completely amorphous and crystalline sample. For PET, ρ_a is 1.335 g/cm^3 (Ref. 8) and ρ_c is 1.455 g/cm^3 (Ref. 9).

Wide Angle X-Ray Scattering (WAXS)

The WAXS analysis of the PET fiber samples were performed on a Siemens type F X-ray diffractometer equipped with goniometer and a proportional counter. Nickel-filtered CuKα radiation with wavelength 1.542 Å was used. The major peaks in the equatorial direction are[9]:

$$(010) \text{ at } 2\theta = 18°$$

$$(\bar{1}10) \text{ at } 2\theta = 23°$$

$$(100) \text{ at } 2\theta = 26°$$

The major peak in the meridional direction is $(\bar{1}05)$ at $2\theta = 43°$.

The X-ray crystallinity K_x was determined using the simplified method proposed by Bosley.[10] The crystallinity index is obtained from the ratio of intensity at 26° to the intensity at 28.6°, for a randomized sample. An index zero is assigned to a value of 1.402 for the intensity ratio and an index 100 when the ratio equals to 2.695.

Apparent crystal sizes were determined from the Scherrer equation,[11] without correcting for lattice distortions:

$$L_{hkl} = \frac{\lambda}{\beta \cos \theta} \tag{2}$$

where L_{hkl} is the average (hkl) interplanar distance, λ is the X-ray wavelength, β is the width at half-maximum intensity of the pure reflection profile in radians, and θ is the Bragg angle. The pure reflection profile for planes (hkl) are obtained from the resolution of the diffraction scan from $2\theta = 10°$ to $2\theta = 40°$ by fitting into three Pearson VII functions,[12,13] corresponding to each one of the major peaks in the equatorial direction.

The determination of the crystalline orientation in PET is complicated by the absence of a true azimuthal reflection (001). The $\bar{1}05$ reflection is the closest to the azimuth, the normal to this plane making an angle of approximately 10° with the c axis.[14] Therefore azimuthal scan with 2θ fixed at 43° is composed of two overlapping components situated at 10° on either side of the meridian. The crystalline orientation factor f_c is defined as

$$f_c = (3\langle \cos^2 \phi_{c,z} \rangle - 1)/2 \tag{3}$$

where $\phi_{c,z}$ is the angle between the fiber axis and the c direction of the unit cell. $\phi_{c,z}$ can be related to $\phi_{\bar{1}05,z}$ from the knowledge of the angle α between the normal to plane $(\bar{1}05)$ and the c direction.

$$\langle \cos^2\phi_{c,z} \rangle = \langle \cos^2\phi_{\bar{1}05,z} \rangle / \cos^2\alpha \quad (4)$$

$$\langle \cos^2\phi_{\bar{1}05,z} \rangle = \frac{\int_0^{\pi/2} I(\phi) \sin\phi \cos^2\phi \, d\phi}{\int_0^{\pi/2} I(\phi) \sin\phi \, d\phi} \quad (5)$$

where $I(\phi)$ is the intensity of the resolved peak at the azimuthal angle ϕ.

Dynamic Mechanical Analysis

Dynamic mechanical measurements were performed with a Rheovibron DDVII-C dynamic viscoelastometer, manufactured by IMASS. This instrument measures the temperature dependence of the complex modulus E^* and tan δ of a viscoelastic solid at a particular frequency. The system includes an Autovibron unit, which controls the heating rate and performs the data acquisition and calculation.

The sample ends are fixed to two clamps, 1 in. apart, and consist of a parallel bundle of fibers with a total of 350 denier. The static stress on the sample was controlled at 0.1 grams/denier (gpd) to minimize dimensional change of the sample during the measurements.[15] The two clamps are attached to strain gauges that monitor the displacement and the dynamic force. A sinusoidal tensile strain is applied to one end of the sample and a sinusoidal stress is generated at the other end of the sample. The phase angle δ between these two sinusoidal waves is read directly from the instrument as tan δ. From the linear viscoelasticity theory,[16] it can be shown that

$$E^* = E' + iE'' \quad (6)$$

where E' is the storage modulus, in-phase with the strain, and E'' is the loss modulus, out-of-phase with the applied strain. Both E' and E'' are related to each other through the ratio

$$\tan\delta = E''/E' \quad (7)$$

The measurements were made at the constant frequency of 11 Hz and in the temperature range of 20–160°C, with heating rate of 1°C/min.

Tensile Test

The ultimate strength and elongation of individual fiber samples were measured in an Instron Tensile Tester model 1122, according to ASTM method D3822-82. The gauge length was 25.4 mm and the crosshead speed was 20 mm/min. The tenacity and elongation to rupture are an average of 10 individual measurements. The denier of the individual fibers was calculated from the measurement of diameter with an optical microscope prior to testing.

Dye Exhaustion

Dye exhaustion experiments were performed on short fibers cut to approximately 1 cm in length. The fibers were dyed in the Ahiba PM Polymat at 100°C with Resolin Blue FBL (CI Disperse Blue 56, molecular weight 349) at the concentration of 3% oil by weight of fiber (o.w.f.), following the procedure described by Kamide et al.[17] A 0.5-mL sample of the dyeing liquor, after 60 and 120 min of dyeing, was dissolved in 10 mL of water–acetone 1:1 mixture and the absorbance of the solution A_t determined at 625 nm in a Perkin-Elmer 559A UV/VIS Spectrophotometer. The dye exhaustion D is then calculated by

$$D = \frac{A_0 - A_t}{A_0} \quad (8)$$

where A_0 is the absorbance of the initial dye solution.

In order to compare fibers with different take-up denier and consequently different surface areas,[18] the value of D was normalized to a round filament of 1 dpf, as suggested in the DuPont patent.[15] On the basis of equivalent surface-to-volume ratio,[15] the normalized dye exhaustion D_n is obtained by

$$D_n = D(\text{dpf})^{1/2} \quad (9)$$

Taut Tie Molecule Fraction

The fraction of taut tie molecule (ttm) is calculated on the basis of the assumption that the modulus of a strained tie molecule is equal to that of a crystal and using the composite model of Takayanagi,[19] with series arrangement of crystalline and amorphous regions coupled in parallel to the fraction of taut tie molecules. The following results[19]:

$$\text{ttm} = \frac{V_a E(E_c - E_a) - E_a(E_c - E)}{V_a E_c(E_c - E_a) - E_a(E_c - E)} \quad (10)$$

where V_a is the volume fraction of the amorphous region and is equal to $1 - K_d$, with K_d obtained from Eq. (1). E is the longitudinal tensile modulus at 25°C, obtained in the Rheovibron. E_c is the crystal modulus along the molecular axis and equal to 110 GPa (856.2 gpd).[20,21] E_a is the modulus of the amorphous region and its value has been reported by Choy et al.[22] as 2.1 GPa (17.8 gpd).

Free Volume

The average volume of the amorphous regions V_{AM} was estimated, assuming an alternating succession of crystalline and amorphous regions, as[23]

$$V_{AM} = V_{CR} \frac{1 - K_d}{K_d} \tag{11}$$

where V_{CR} is the average volume of a crystal. V_{CR} can be estimated from the two lateral crystal sizes and the longitudinal one, according to the following relation:

$$V_{CR} = \frac{L_{100}}{a} \frac{L_{010}}{b} \frac{L_{\bar{1}05}}{c} V_u \tag{12}$$

Daubeny et al.[9] reported the values of a, b, and c, the unit cell dimensions of the PET crystal structure, as 4.56, 5.94, and 10.75 Å, respectively. V_u, the volume of the unit cell, was estimated as 219 Å^3.

Vassilatos et al.[24] calculated the free volume V_f, correcting the expression (11) for the tortuosity of the diffusional paths as follows:

$$V_f = V_{AM} \frac{1 - f_a}{f_a} \tag{13}$$

where f_a is the Herman orientation function for the amorphous regions, which can be determined from the birefringence measurements. Applying the superposition principle proposed by Stein and Norris,[25] one obtains

$$\Delta n = K_d f_c \, \Delta n_c + (1 - K_d) f_a \, \Delta n_a \tag{14}$$

Δn_c and Δn_a are the intrinsic birefringence of the crystalline and amorphous phase, respectively. Dumbleton[26] reported Δn_c as 0.220 and Δn_a as 0.275.

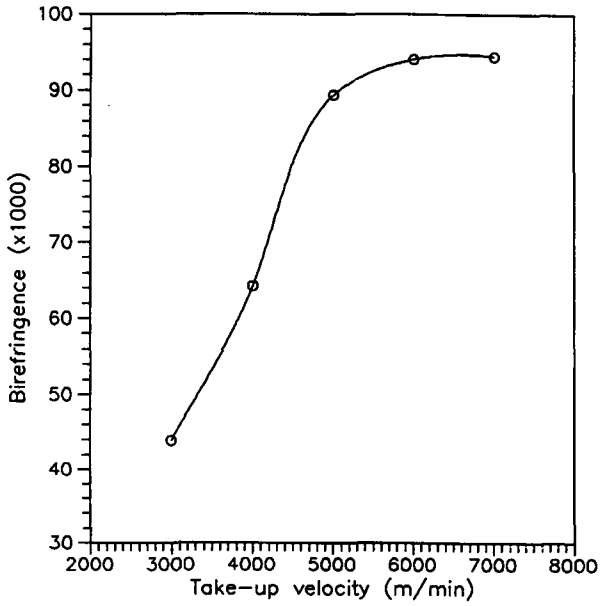

Figure 1 Birefringence of 1 dpf fibers as a function of take-up speed.

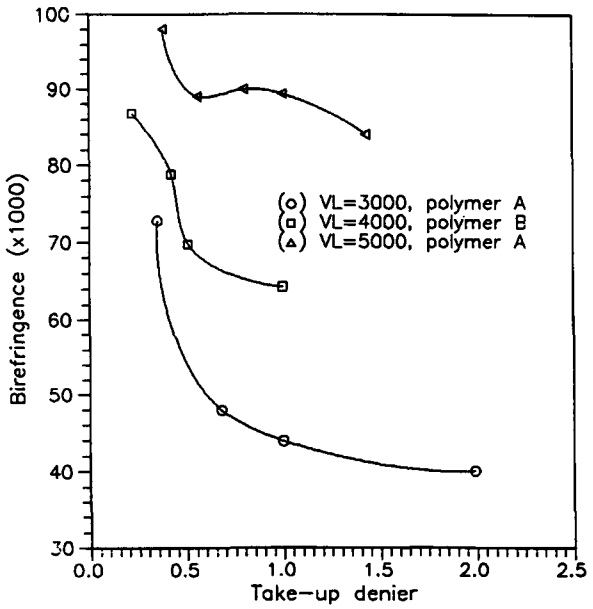

Figure 2 Birefringence as a function of take-up denier for different spinning speeds.

RESULTS AND DISCUSSIONS

Effect of Take-up Speed and Denier on the Orientation and Crystallization Behavior of PET Fibers

Figure 1 shows the increase of birefringence with increase of the take-up speed, where the take-up denier was constant and equal to 1 dpf. Up to 5000 m/min, the birefringence increases sharply but approaches a plateau at the speed of 7000 m/min. Figure 2 shows the effect of take-up denier on the birefringence results, at take-up speeds of 3000, 4000,

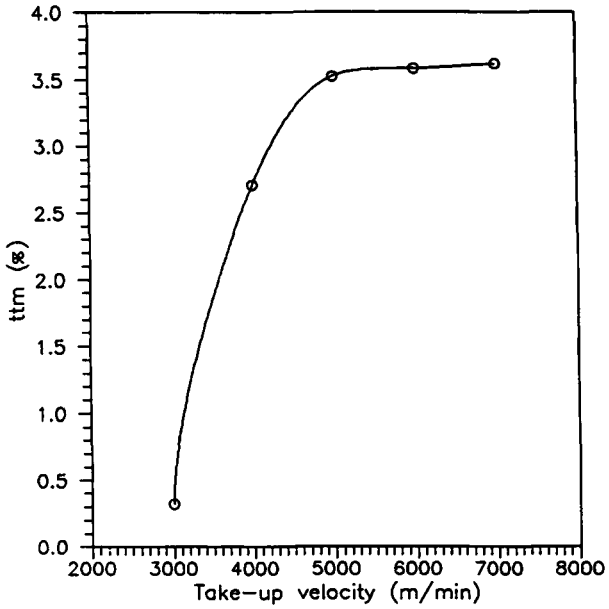

Figure 3 Fraction of taut tie molecules of 1 dpf fibers as a function of take-up speed.

and 5000 m/min. These curves show a sharp increase of the birefringence with the reduction of take-up denier, particularly for take-up denier below 0.5 dpf. At the speed of 5000 m/min, the birefringence increases slower with decrease of take-up denier than it does at lower speeds, consistent with the birefringence approaching a plateau shown in Figure 1 at speeds greater than 5000 m/min. However, the birefringence of the finest denier fibers spun at 5000 m/min still exceeds the birefringence of the 1 dpf fiber spun at a speed 2000 m/min higher, i.e., at 7000 m/min.

The saturation of the birefringence at the take-up speed near 7000 m/min, shown in Figure 1, has been well documented in the literature.[24,27-29] This phenomenon has been explained on the basis of a selective crystallization mechanism, by which the oriented molecules are incorporated into the crystalline phase, resulting in a more disoriented amorphous phase.[29] This view is consistent with the results of the fraction of taut tie molecules, shown in Figure 3. The ttm fraction increases with the increase of the take-up speed up to 5000 m/min and remains almost constant in the range of speed from 5000 to 7000 m/min. The sharp increase of take-up tension, presented in the earlier paper,[5] with the increase of take-up speed therefore is not accompanied by a proportional increase of orientation.

The increase of the birefringence, at all take-up speeds from 3000 to 5000 m/min, with the reduction of the take-up denier is also consistent with the increase of the fraction of taut tie molecules with the decrease of take-up denier, presented in Figure 4. The increase of birefringence with the decrease of take-up denier might be seen as analogous to the phenomenon of birefringence increase with the increase of take-up velocity. Take-up tension also increases sharply with decrease of take-up denier, as shown in the earlier study.[5] These results are expected from the increase of the air drag contribution to the spinline tension due to increased cooling rate.[30] However, the birefringence values shown in Figure 2 do not present a trend of saturation as the take-up denier decreases. The birefringence of the 0.38 dpf fibers spun at 5000 m/min is even higher than the maximum birefringence of the 1 dpf fibers, which is obtained at 7000 m/min. If the effect of decreasing dpf were the same as increasing speed, one would expect that at 5000 m/min, any decrease of dpf or increase of the speed would have little effect or even decrease of the birefringence, based on the results of Figure 1. However, this distinct behavior can be explained with the results of the threadline dynamics discussed in Part II.[5] It was shown that the maximum velocity gradient increases faster with the decrease of the take-up denier than it does with the increase of take-up speed. Since the velocity gradient in the threadline is responsible for the alignment of the molecules, higher birefringence can be expected from higher velocity gradient.

The results of crystallinity index determined by WAXS and density are shown in Figures 5 and 6.

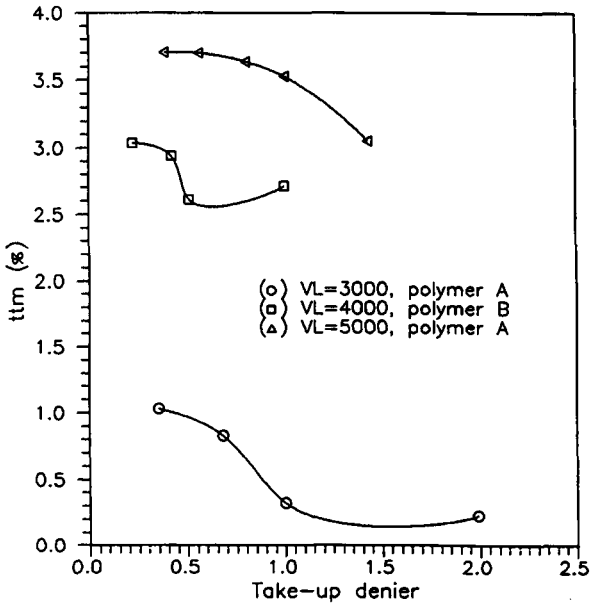

Figure 4 Fraction of taut tie molecules as a function of take-up denier for different spinning speeds.

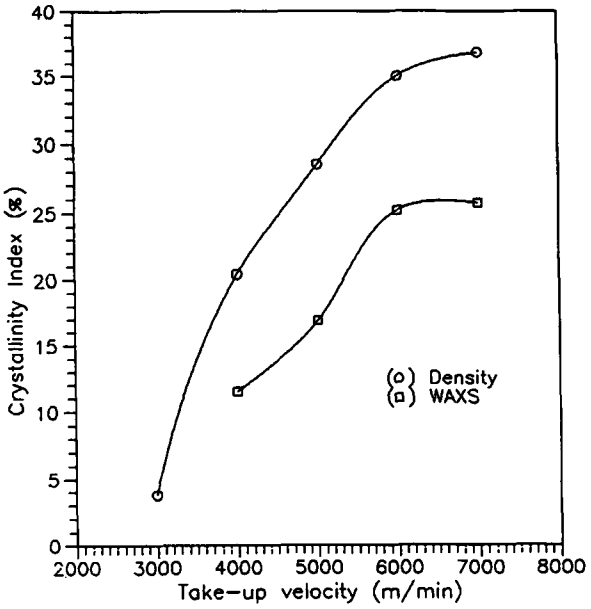

Figure 5 Crystallinity index determined from WAXS and density as a function of take-up velocity. dpf = 1.00.

The crystallinity determined by WAXS is zero for the fibers spun below 3000 m/min. Both methods indicate an increase of the crystallinity of the 1 dpf fibers with increasing take-up speed up to 7000 m/min, as shown in Figure 5. A maximum in crystallinity as a function of take-up denier is observed at the speeds of 4000 and 5000 m/min. The maximum is observed with WAXS and density, and it appears at the take-up denier of 0.5 dpf for fibers spun at 4000 m/min, and at the take-up denier of 0.8 dpf for fibers spun at 5000 m/min. No crystallinity maximum is observed at the speed of 3000 m/min, where the crystallinity index increases only slightly and continuously with the decrease of the take-up denier.

Figure 7 shows that the crystal size increases in both width and in length as the take-up speed increases. $L_{\bar{1}05}$ increases linearly with the take-up speed while the increase in L_{010} is almost parallel to the increase in L_{100}. A broad maximum of crystal size as a function of the take-up denier can be seen in Figure 8 for fibers spun at 4000 m/min. The maximum is observed around the take-up denier of 0.5 dpf. At 5000 m/min, a sharper maximum occurs in $L_{\bar{1}05}$ versus take-up denier near 0.8 dpf, as shown in Figure 9. The crystal widths show a less pronounced maximum, even indicating a trend of increasing crystal width with decreasing take-up denier of fibers spun at 5000 m/min. Figure 10 presents data of $L_{\bar{1}05}$ at 4000 and 5000 m/min as a function of take-up denier. These data include different types of PET polymers and spinning conditions, which result in the greater scatter of the plots. However, a maximum in $L_{\bar{1}05}$ can be visualized at both take-up speeds for denier in the range of 0.5–1.0 dpf.

The trend indicated by the crystallinity index versus the take-up velocity, shown in Figure 5, is in accord with the results from the literature.[24,27–29] The

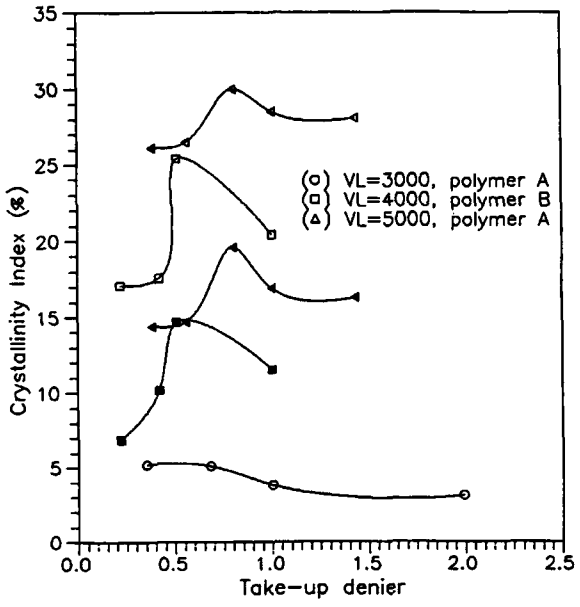

Figure 6 Crystallinity index determined from WAXS (filled symbols) and density (unfilled symbols) as a function of take-up denier.

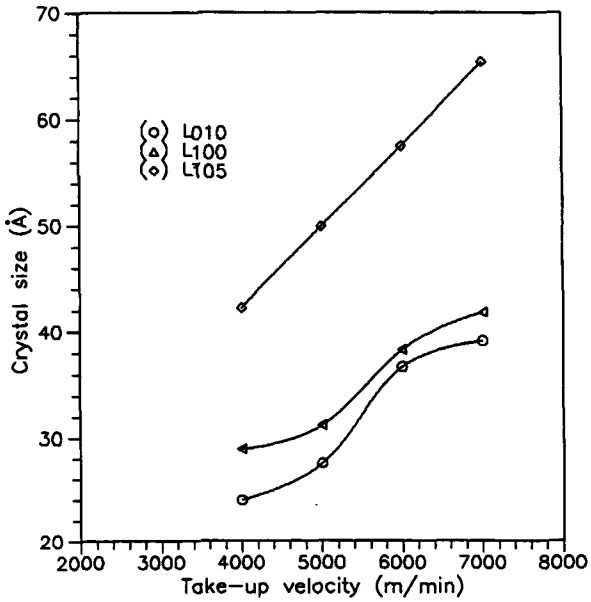

Figure 7 Crystal size as a function of take-up velocity, for 1 dpf fibers.

slower increase of the crystallinity at higher speeds and eventually a reduction of the crystallinity at even higher speeds has been theoretically analyzed by Ziabicki.[30] Ziabicki predicted that a maximum in the crystallinity index versus take-up velocity would occur due to the compromise between the increase in orientation and the decrease in crystallization time as the take-up speed increases.

In the spinning of finer denier fibers, the cooling rate is increased significantly, as discussed in the previous paper,[5] and the time allowed for the crystallization process is reduced dramatically. Yasuda[31] explained the decrease of the density and the maximum of crystal size with decrease of mass flow rate at 6000 m/min as a result of the shorter residence time in the temperature interval where the maximum crystallization rate occurs. Matsui[6] and Fujimoto et al.[32] attributed the crystallinity suppression, as the take-up denier is reduced, primarily to the occurrence of cold drawing by destroying the nucleated crystal structure. Our results show that the maximum crystallinity of fibers spun at 5000 m/min occurs at the take-up denier of approximately 0.8 dpf, while at 4000 m/min the crystallinity maximum is observed at a lower take-up denier near 0.5 dpf. At 3000 m/min, no WAXS can be obtained. However, the crystallinity from density and WAXS, although different in magnitude, shows similar trends. Therefore at 3000 m/min, a maximum in crystallinity is not observed or would occur outside the range of denier studied, below 0.3 dpf. It can be

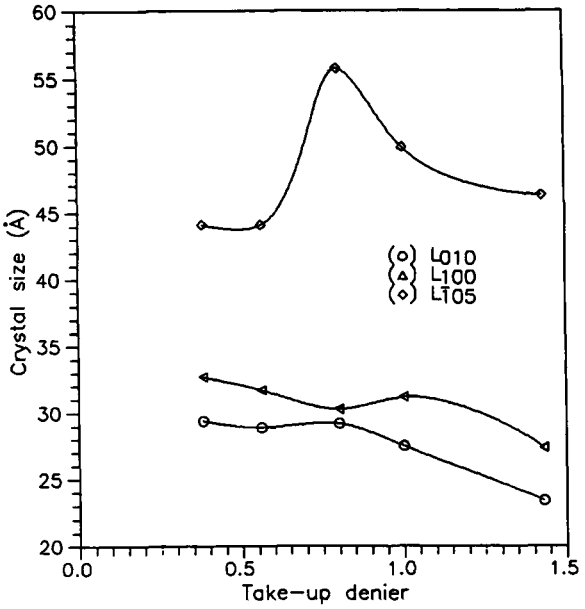

Figure 9 Crystal size of polymer A as a function of take-up denier, spun at 5000 m/min.

realized that the maximum crystallinity shifts to higher take-up denier as the take-up velocity increases. This result contradicts the conclusion of Matsui[6] and Fujimoto et al.[32] who attributed the crystallinity suppression to the occurrence of cold drawing. As shown by their results and our own data,[5] fibers spun at lower speeds are more vulnerable to cold drawing due to the less well developed

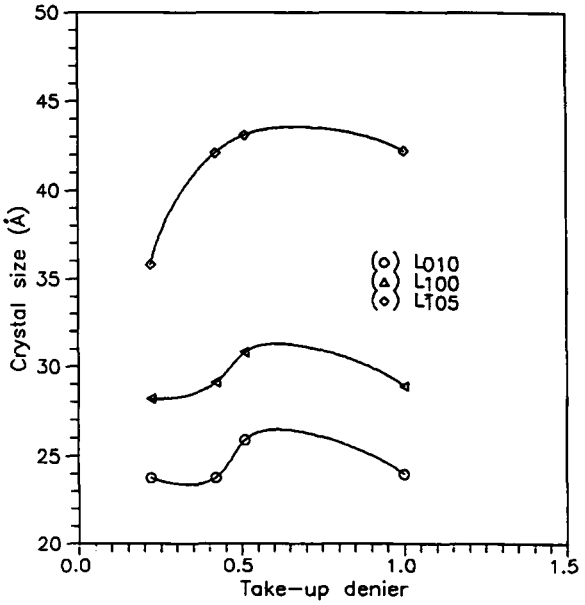

Figure 8 Crystal size of polymer B as a function of take-up denier, spun at 4000 m/min.

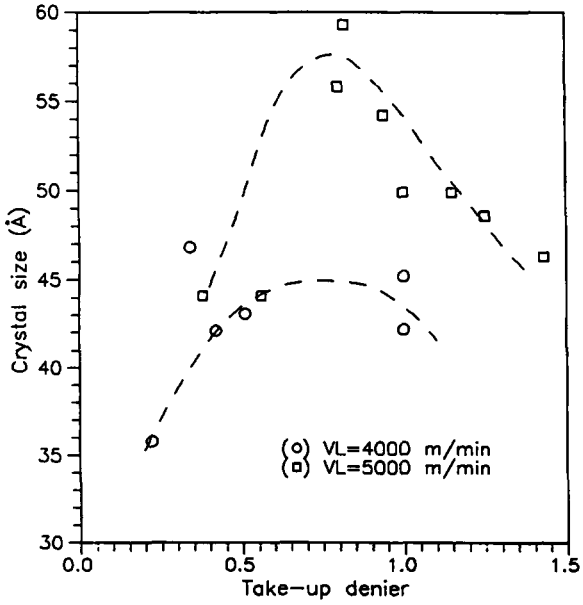

Figure 10 Overall correlation of crystal size ($L_{\bar{1}05}$) with take-up denier at different spinning speeds.

crystal structure. Yet our results indicated that the usual conditions employed in the spinning of fine denier fibers does not cause cold drawing.[5] Moreover, the fibers spun at higher speeds were shown to present maximum crystallinity at higher take-up denier, contrary to what is expected from the phenomenon of cold drawing. The shift of the maximum crystallinity to higher take-up denier with increasing speeds could be related to the rapid increase of the take-up tension when decreasing take-up denier, particularly at higher take-up speeds, as discussed in Part II.[5] The role of the stress is unclear, but it seems possible that high stress prevents crystal growth as opposed to destruction.[30,33] More likely, this shift is related to decreasing crystallization time with decreasing take-up denier or increasing velocity, i.e., for comparable crystallization time, a decrease of the take-up denier should be followed by a decrease in the take-up velocity.

The reduced time allowed for crystallization can also explain the continuous increase of the birefringence at 5000 m/min with reduction of the take-up denier, discussed earlier. As already mentioned, the reduction of birefringence results from the selective crystallization mechanism by depletion of the more oriented molecules in the amorphous region, which is incorporated onto the crystal. If there is not enough time for the incorporation of the oriented molecules to the crystalline region, the latter is prevented from growing and the orientation of the amorphous region is preserved. Data on crystal size shown in Figures 8–10, particularly $L_{\bar{1}05}$, substantiate this approach. The data in Figure 10 show that the curves of $L_{\bar{1}05}$ versus take-up denier show a maximum, in accord with the results reported by Yasuda,[31] clearly indicating that crystals were prevented from growing due to the limited time available for crystallization. Maximum of crystal size was not observed as a function of take-up speed, confirming that the increase of the spinline tension at higher speeds had no effect in restraining crystal growth. The continuous increase of the crystal size with the take-up velocity, shown in Figure 7, has been reported by other authors[34,35] and attributed to the lower degree of supercooling at higher take-up velocity.[34]

Effect of Take-up Speed and Denier on the Thermal Properties of PET Fibers

The results of the thermal analysis in the DSC are shown in Figures 11 and 12. Figure 11 presents the effect of the take-up speed. T_g is not observed at the take-up speed of 5000 m/min. The crystallization

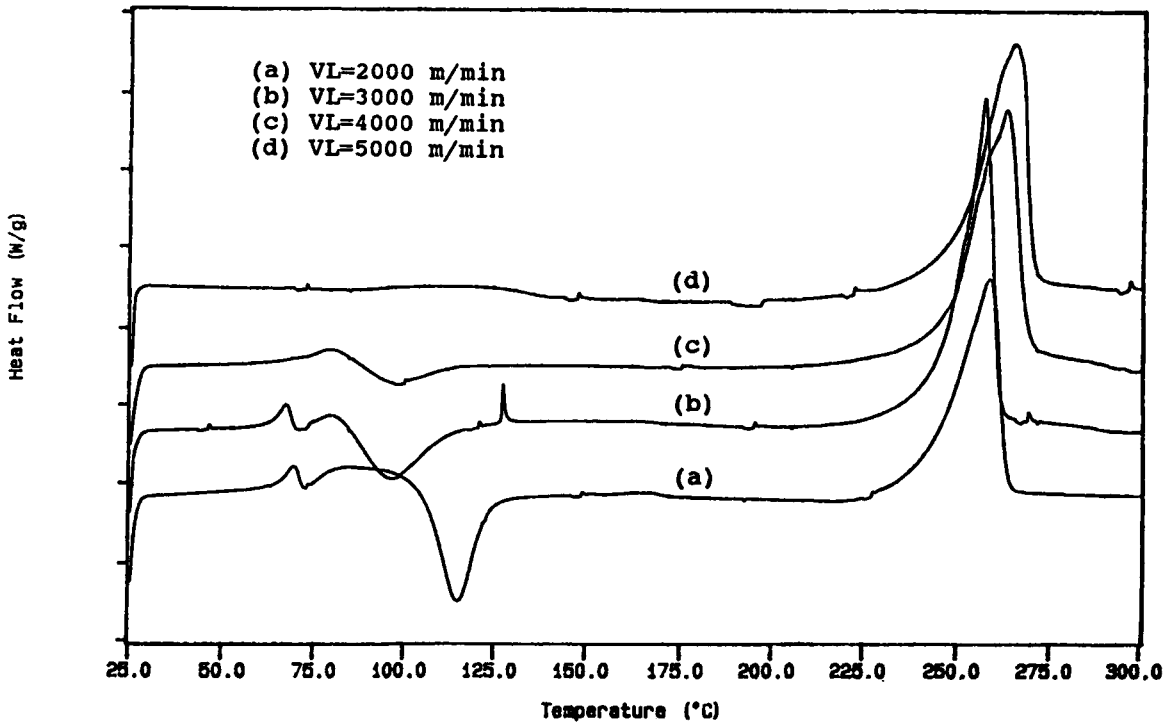

Figure 11 DSC curves of polymer A as a function of take-up velocity (heating rate = 10 K/min). L = 1.6 m, dpf = 1.00, without quench/heating.

peak shifts to lower temperatures and its intensity decreases when the speed increases. At 5000 m/min, the crystallization peak disappears. The temperature and area of the melting peak increase with increasing take-up speed and a shoulder appears at the speed of 4000 m/min in the melting peak, which corresponds approximately to the position of the melting peak of the fibers spun at lower speeds. The effect of take-up denier, at the constant speed of 3000 m/min, is shown in Figure 12. It can be seen that as the take-up denier decreases, the glass transition temperature becomes sharper and shifts to lower temperatures, the crystallization peak temperature decreases as well as its intensity. The melting peak narrows and its intensity increases.

The effect of reducing the take-up denier is shown to be similar to the increase of take-up velocity on the DSC profiles, particularly the shift of the crystallization peak to lower temperatures. The effect of the take-up speed on the DSC thermographs is consistent with the data found in the literature,[27,34] which also reported that the cold crystallization peak temperature and the peak area decreases with the increase of speed, disappearing at speeds above 5000 m/min. These authors,[27,34] however, do not mention the presence of the shoulder in the melting peak, observed in our data particularly at 4000 m/min. Double endotherm peaks have been attributed to the melting of ordered small regions due to annealing of the sample during testing,[36,37] and does not occur in samples not allowed to shrink during the DSC test.[38] The appearance of the shoulder in the endotherm peak at the speed of 4000 m/min, however, seems to be related to a transition toward better crystallized samples in fibers spun at 5000 m/min. This is indicated by the coincidence of the shoulder temperature with the melting peak of the fibers spun at 3000 m/min, while the major peak coincides with the higher melting peak of the fibers spun at 5000 m/min. This reasoning is also confirmed by the absence of double endotherm peak for the different take-up denier fibers spun at 3000 m/min, since at this speed no diffraction patterns was observed even for the finest denier fibers.

Dynamic-Mechanical Properties of Fine Denier PET Fibers Obtained in High-Speed Melt Spinning

The effect of the take-up speed on the maximum of tan δ as well as the temperature at which the maximum occurs is shown in Figure 13. The height of the tan δ peak decreases continuously with the increase of the take-up velocity up to 6000 m/min, remaining almost constant with further increase of

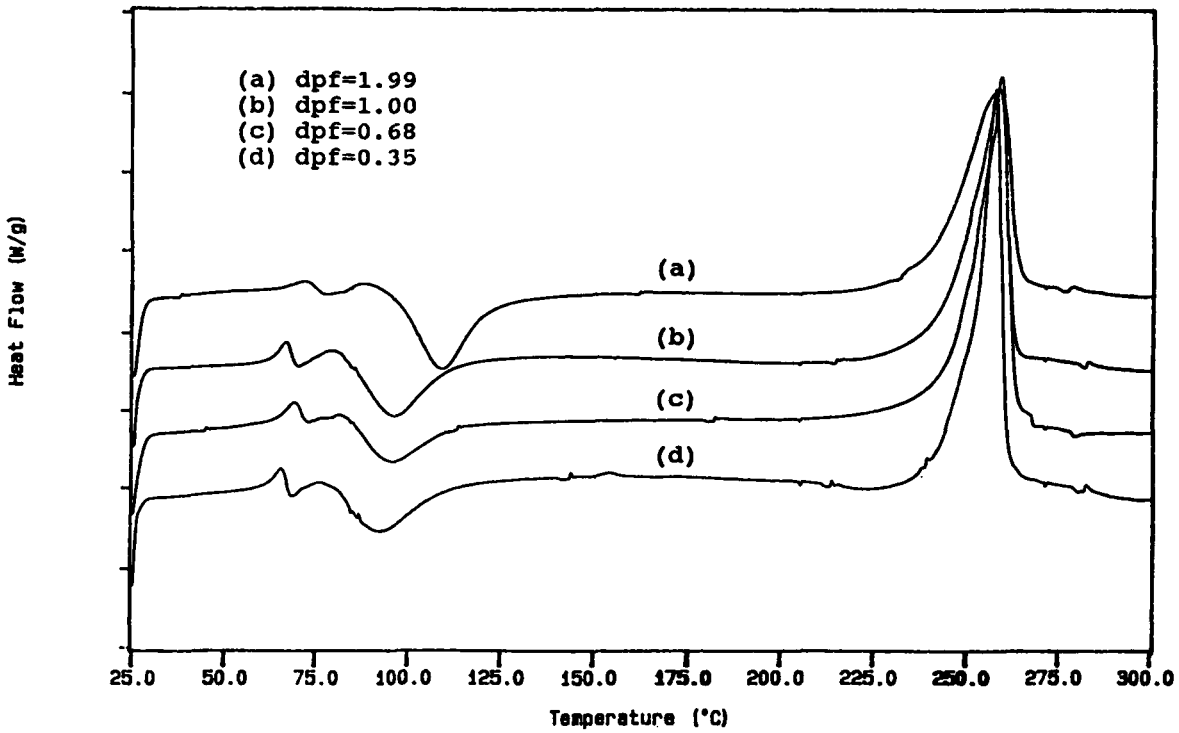

Figure 12 DSC curves of polymer A as a function of take-up denier (heating rate = 10 K/min). L = 2.6 m, V_L = 3000 m/min, without quench/heating.

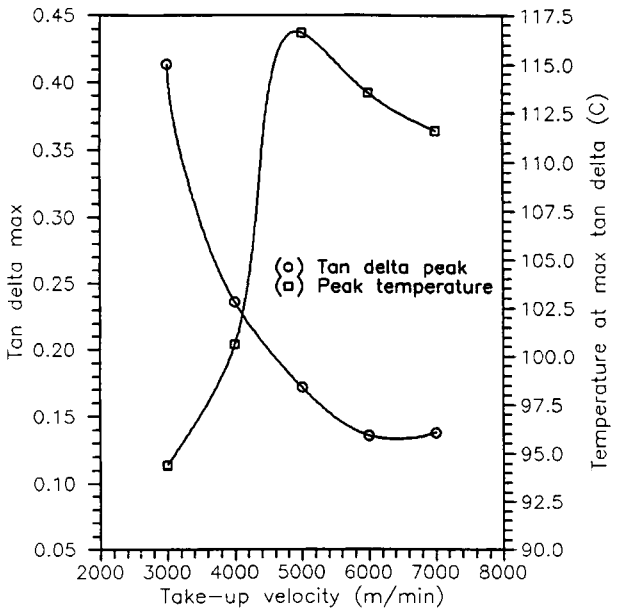

Figure 13 Effect of take-up velocity on the tan δ peak and temperature of the peak. dpf = 1.00.

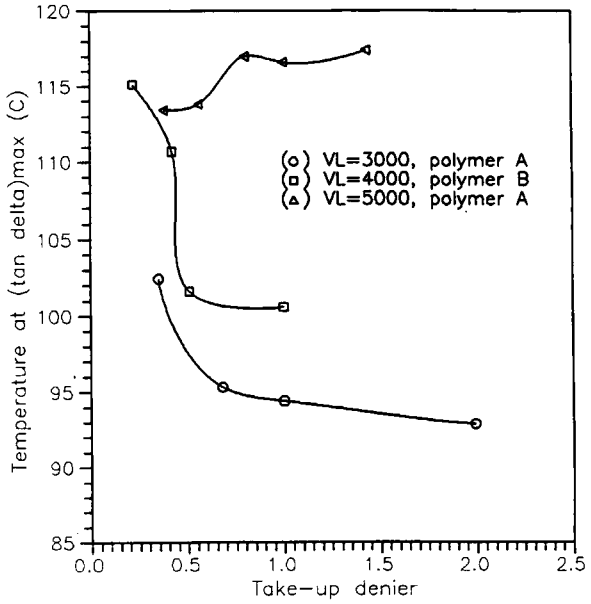

Figure 15 Effect of take-up denier on the temperature of tan δ peak, at different spinning speeds.

the speed to 7000 m/min. On the other hand the tan δ peak temperature goes through a maximum with the take-up velocity around 5000 m/min. Figure 14 shows that the height of the tan δ peak decreases with the decrease of the take-up denier at the speeds of 3000 and 4000 m/min. At 5000 m/min, the height of the tan δ peak is slightly reduced when the take-up denier decreases. Figure 15 shows that the temperature at which the tan δ is maximum increases as the take-up denier decreases, at the take-up speeds of 3000 and 4000 m/min. The reverse occurs at the speed of 5000 m/min, where the tan δ peak temperature shows a slight maximum and then decreases with the decrease of the take-up denier.

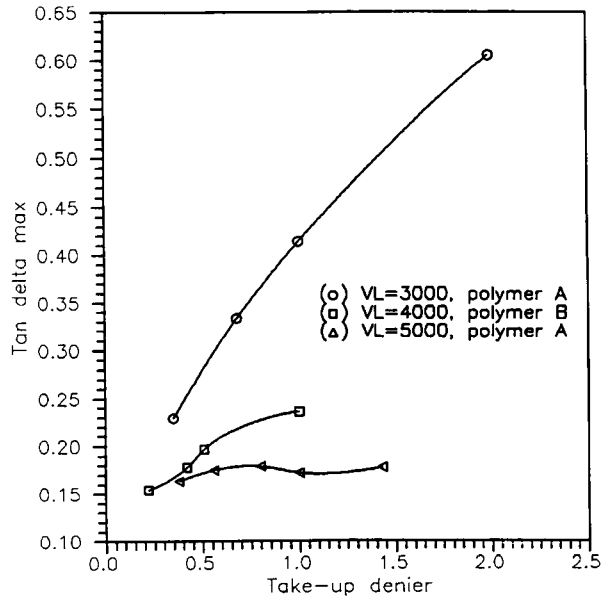

Figure 14 Effect of take-up denier on the tan δ peak, at different spinning speeds.

The results presented in Figure 13 are consistent with those presented by Kamide et al.[39] The dynamic loss tangent was shown in Eq. (7) to be the ratio between the loss to storage modulus. This ratio can also be interpreted as the fraction of energy lost per cycle due to viscous dissipation caused by friction of molecules during chain segment motion. Therefore any restrictions to segment mobility, and thereby reduction of chain slippage, should reduce the magnitude of δ or require higher energy to effect the motion. Manabe and Kamide,[40] using a spring and bead representation for the molecules in the amorphous region, derived a mathematical model to predict the temperature dependence of tan δ. In this model the maximum value of tan δ is related to the volume fraction of the amorphous region, while the temperature of the maximum tan δ is related to the molecular packing density of the amorphous region. A peak broadening can then be interpreted as the consequence of a distribution of the molecular packing density in the amorphous regions. Since the presence of crystals can also act as crosslinks, restricting segment mobility, Murayama[23] also points out the effect of crystal size and number on the tan δ peak. Few large crystals have less effect in re-

straining the motion of chains than a large number of small crystals.

The decrease of tan δ at all take-up speeds up to 7000 m/min can then be explained by the increase of the birefringence and crystallinity index, shown in Figures 1 and 5, respectively. The temperature at which the maximum of tan δ occurs should correlate with the calculated free volume. The free volume, as discussed in the experimental section, takes into account the crystal size and volume fraction as well as the orientation in the amorphous region. Figure 16 shows that the free volume goes through a minimum at the take-up velocity of 5000 m/min. It can be seen that up to 5000 m/min, the free volume decreases, therefore restraining the segmental motion due to an increased packing density, which shows up as a shift of the tan δ peak to higher temperatures. Above 5000 m/min, the free volume increases, and consequently the peak temperature decreases. The correlation between free volume and the temperature at which the loss modulus E'' is maximum has been reported elsewhere.[24,41] The loss modulus peak is affected in a similar manner as is the tan δ peak, however, the tan δ peak has the advantage of not being dependent on the sample dimensions.

The same reasoning may be applied to explain the effect of the take-up denier on the temperature dependence of tan δ. Figure 14 shows that the tan δ peak decreases as the take-up denier decreases, at

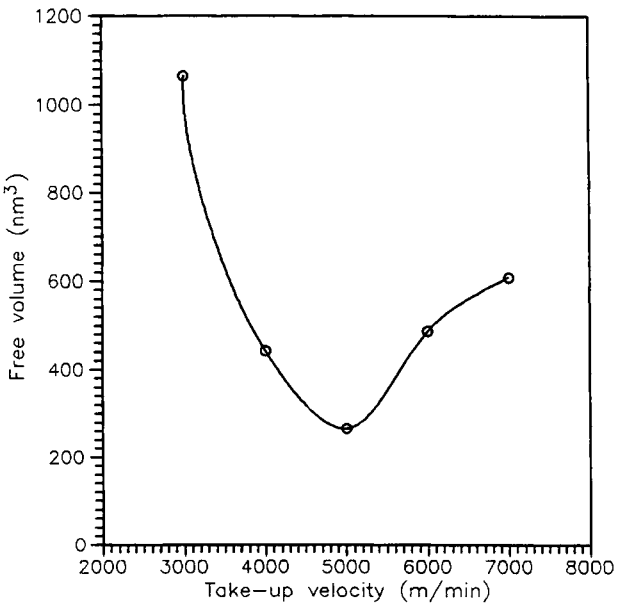

Figure 16 Effect of take-up velocity on free volume of 1 dpf fibers. Free volume corrected for tortuosity in amorphous regions.

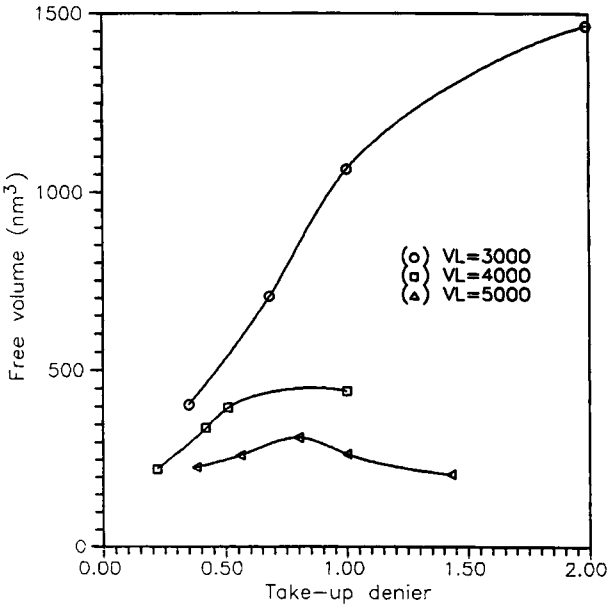

Figure 17 Effect of take-up denier on free volume for different spinning speeds. Free volume corrected for tortuosity in amorphous regions.

all speeds from 3000 to 5000 m/min, which can be explained by the increase of the birefringence shown in Figure 2. The crystallinity maximum shown in Figure 6 had no apparent effect on the tan δ curves, or more likely it may have been offset by the continuous increase of the fiber orientation (birefringence, ttm fraction). The results of tan δ peak temperature, shown in Figure 15 as a function of the take-up denier, can also be successfully explained by the results of free volume shown in Figure 17. At speeds lower than 5000 m/min, a decrease of the take-up denier decreases the free volume, and consequently the tan δ peak temperature increases. At 5000 m/min, the effect of decreasing take-up denier on the free volume and peak temperature is reversed. The tan δ peak temperature decreases slightly while the free volume shows a small maximum, when the take-up denier decreases at 5000 m/min.

Tensile Properties of Fine Denier PET Fibers Obtained in High-Speed Melt Spinning

Figure 18 shows that the tenacity of the 1 dpf fibers increases with increase of the take-up velocity up to 5000 m/min and then decreases with further increase of the speed to 7000 m/min. The elongation to rupture decreases with the take-up velocity in the whole range of speeds tested, from 3000 to 7000 m/min. The maximum attainable tenacity was ap-

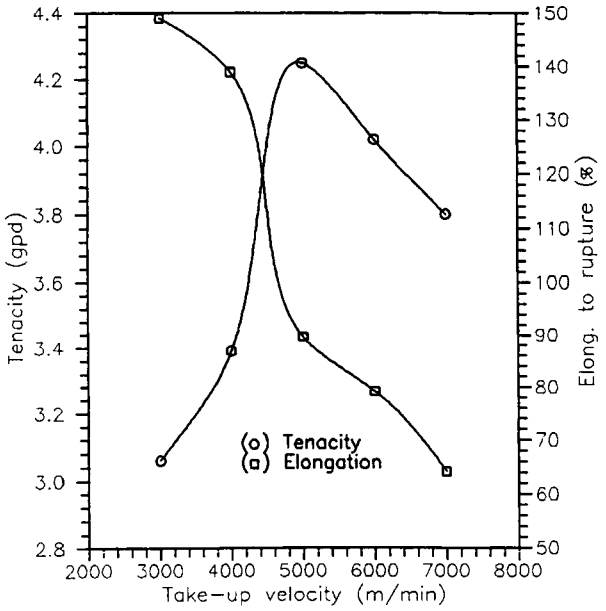

Figure 18 Effect of take-up velocity on tenacity and elongation to rupture of 1 dpf fibers.

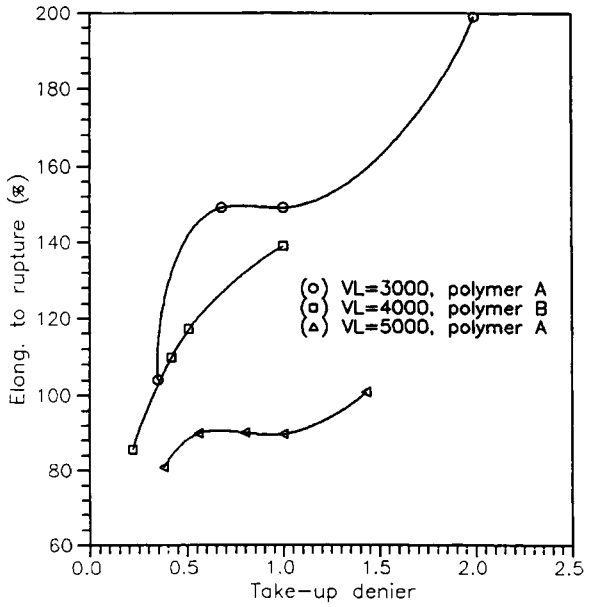

Figure 20 Elongation to rupture as a function of take-up denier, at different spinning speeds.

proximately 4 gpd whereas the minimum attainable elongation to rupture was around 60%.

The influence of the take-up denier on the fiber tenacity is shown in Figure 19. Tenacity increases as the take-up denier decreases, for the take-up speeds of 3000 and 4000 m/min. At 5000 m/min, the tenacity shows a slight maximum around the take-up denier of 0.8 dpf. Figure 20 presents the results of the elongation to rupture as a function of take-up denier. At all speeds in the range of 3000–5000 m/min, the elongation to rupture is shown to decrease with the decrease of the take-up denier. The decrease of the take-up denier at 5000 m/min has small effects on the decrease of the elongation to rupture, the latter being always larger than 80% even for the finest denier.

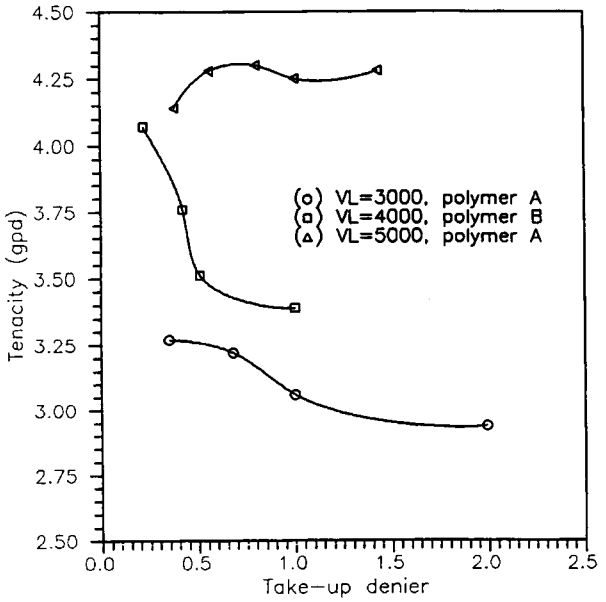

Figure 19 Tenacity as a function of take-up denier, at different spinning speeds.

It can be seen in Figures 18 and 20 that the reduction of the take-up denier has the same effect as an increase of the take-up speed on the decrease of the ultimate elongation. The decrease of the ultimate elongation is the result of increased orientation as determined by the birefringence or ttm fraction. The maximum in tenacity, observed at the take-up speed of 5000 m/min for the 1 dpf fibers, has been reported to occur in the range of 5000 to 6000 m/min,[27,28] and has been attributed to the radial differentiation of the structure, which increases with the increase of take-up speed.[28] The effect of decreasing take-up denier on tenacity, shown in Figure 19, is analogous to the effect of increasing take-up velocity. At speeds lower than 5000 m/min, tenacity increases with the decrease of take-up denier in a way similar to the increase of the take-up velocity, and can be attributed to the increase of birefringence and ttm fraction. At 5000 m/min the decrease of take-up denier leads to a slight decrease of tenacity, which is expected from the results of Figure 18 if a decrease in the take-up denier is equivalent to an increase of take-up velocity. The decrease of the tenacity with

the decrease of the take-up denier at 5000 m/min is not as large as one would expect from the results in Figure 18, possibly due to partial compensation by the increase of the ttm fraction, shown in Figure 4.

Effect of Take-up Speed and Denier on the Dye Exhaustion Properties of PET Fibers

The results of the dye exhaustion experiments are shown in Figures 21 and 22. Dye exhaustion goes through a minimum at the speed of 5000 m/min, as shown in Figure 21. Increasing the dyeing time reduces the differences of dye exhaustion due to the different take-up velocity, mainly due to the increased exhaustion by the fibers spun at speeds greater than 4000 m/min. However, the minimum of dye exhaustion can still be recognized at the speed of 5000 m/min. The effect of the take-up denier on dye exhaustion is shown in Figure 22. Dye exhaustion decreases as the take-up denier decreases. It should be emphasized that the observed differences are not a consequence of the difference in surface area, since the dye exhaustion results have been normalized to the equivalent surface area of the 1 dpf fiber, as discussed in the experimental section. It can also be observed in Figure 22 that the dye exhaustion of fibers spun at 5000 m/min decreases slower than the dye exhaustion of fibers spun at 4000 m/min. A cross-over point can be observed near 0.8 dpf, below which the dye exhaustion of fibers spun at 5000 m/min becomes higher than that of fibers spun at 4000 m/min.

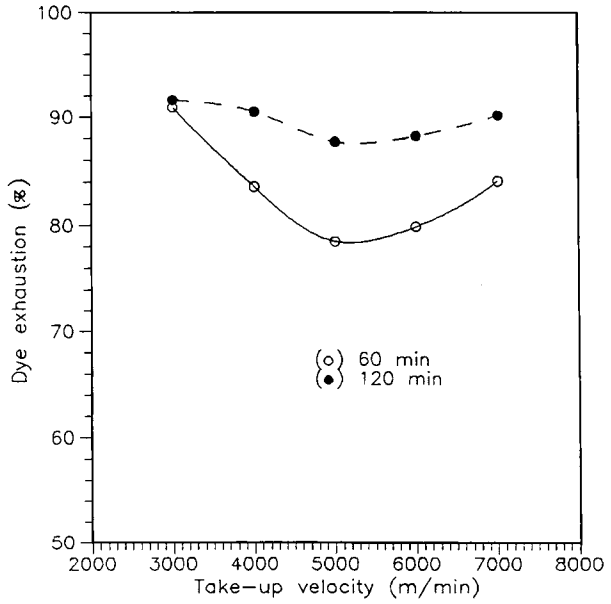

Figure 21 Effect of take-up velocity on dye exhaustion of 1 dpf fibers at 100°C and different time as indicated. Dye Resolin Blue FBL (CIDB 56), 3% o.w.f.

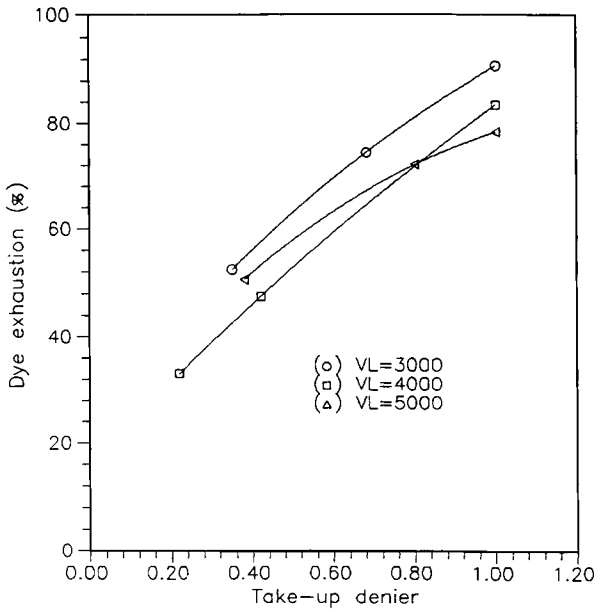

Figure 22 Effect of take-up denier on dye exhaustion (normalized to 1 dpf fibers), 60 min at 100°C. Dye Resolin Blue FBL (CIDB 56), 3% o.w.f.

The minimum dye exhaustion of the 1 dpf fibers, observed at 5000 m/min, is in accord with the results reported by Kamide et al.[17] This result is also consistent with the minimum free volume as well as the maximum of the tan δ peak temperature observed at 5000 m/min for the 1 dpf fiber, as discussed earlier.

The results of dye exhaustion represent an independent confirmation of the increase of mobility of the chain segments in the amorphous regions when 1 dpf fibers are spun at speeds above 5000 m/min. It is interesting to note that study of dye diffusion rate in nylon 66 with the same dyestuff (CI disperse blue 56) also showed a minimum at 5000 m/min.[42] The effect of decreasing take-up denier is to reduce the dye exhaustion rate and can also be explained by the free volume and tan δ peak temperature. The reversal of the effect of take-up denier at 5000 m/min on free volume and temperature of tan δ peak, discussed earlier, can explain the slower decrease of the dye exhaustion with the decrease of the take-up denier as compared to the effect observed at 3000 and 4000 m/min. A general trend can be visualized in Figure 23 of the relation between dye exhaustion and chain mobility, expressed by the temperature of the tan δ peak and the free volume. Higher chain mobility, indicated by higher free vol-

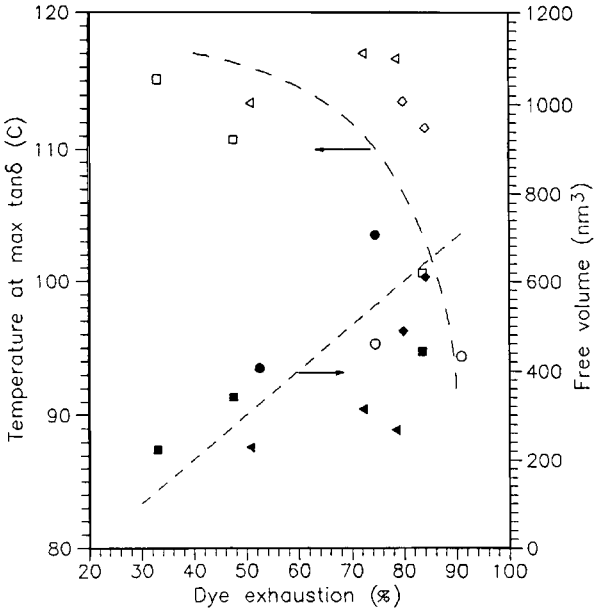

Figure 23 Overall correlation of dye exhaustion (Resolin Blue FBL 100°C/60 min) with temperature of tan δ peak (unfilled symbols) and free volume (filled symbols).

ume or lower tan δ peak temperature, allows higher dye exhaustion as expected.[24]

CONCLUSIONS

The effect of decreasing take-up denier on the structure and mechanical properties of as-spun PET fibers can be shown to be, in general, similar to an increase of take-up velocity. Both can be related to increased threadline cooling rate and increased spinline stress, which control the structure development in the threadline.

DSC analysis showed that the cold crystallization peak can be shifted to lower temperature, and its intensity can be reduced by either an increase of the take-up velocity or decrease of the take-up denier. Tenacity and elongation are also affected similarly by an increase of the velocity or a decrease of the denier.

However, a close analysis of the birefringence and crystallization data showed that the correspondence between denier decrease and velocity increase is no longer applicable. A continuous increase of birefringence is observed with decrease of the take-up denier while a plateau is obtained with increase of take-up velocity. A maximum in crystallinity and crystal size was observed with the take-up denier but not with the take-up velocity. The distinct effect on the birefringence results was explained on the basis of a larger effect of the take-up denier on the maximum of the velocity gradient than the change of the velocity gradient due to the take-up velocity, according to the results of the threadline dynamics presented in the previous paper.[5] Higher velocity gradients can develop higher molecular orientation. Since the maximum velocity gradient is dependent on the threadline cooling rate, it is deduced that in the range of take-up denier (0.2–2.0 dpf) and take-up velocity (2000–7000 m/min) studied, the variation of the take-up denier has the largest effect on the cooling rate. The higher cooling rate, and therefore the shorter time in the temperature range where the crystallization rate is maximum, is considered as the major parameter to explain the maximum in crystallinity as a function of take-up denier. Due to the short time available, the more oriented molecules remain in the amorphous region, which would otherwise be incorporated to the crystalline phase according to Ziabicki's selective crystallization mechanism. Consequently the orientation of the amorphous regions can be preserved or even increased, which is confirmed by the continuous increase of the birefringence with the decrease of the take-up denier. In the literature the crystallinity suppression has also been attributed to the destruction of the crystalline structure by a cold-drawing process; however, this approach is in conflict with our results and cannot explain the observed shift of the maximum crystallinity and crystal size to higher values of take-up denier as the take-up velocity increases. These results have been successfully explained on the basis of the available time for the crystallization process.

Other properties, however, cannot be related to the individual structure parameters just discussed. The intensity of the tan δ peak is related to the volume fraction and orientation of the amorphous regions. The temperature at which the tan δ is maximum as well as the dye uptake depend on the free volume. The free volume takes into account the volume fraction and orientation of the amorphous phase as well as the crystal size. The effect of take-up denier or velocity are therefore the resultant of the overall changes in structure, which may or may not be affected in a similar way by the decrease of denier or increase of the velocity.

The authors wish to acknowledge the financial support received from Rhodia S.A.

REFERENCES

1. *JTN*, **387**, 46–53 (1987).
2. W. L. Anderson, 12th Technical Symposium, Asso-

ciation of the Nonwoven Fabrics Ind., 1984, pp. 265–276.
3. S. Davies, *Textile Horizons,* **8**(4), 49–50 (1988).
4. P. V. Alston, *Textile Res. J.,* **60,** 303–305 (1990).
5. C. T. Kiang and J. A. Cuculo, *J. Appl. Polym. Sci.,* **46,** 67–82 (1992).
6. M. Matsui, in A. Ziabicki and H. Kawai, Eds., *High Speed Fiber Spinning,* Wiley, New York, 1985, Chapter 5.
7. C. T. Kiang and J. A. Cuculo, *J. Appl. Polym. Sci.,* **46,** 55–65 (1992).
8. G. Farrow and I. M. Ward, *Polymer,* **1,** 330–339 (1960).
9. R. P. Daubeny, C. W. Bunn, and C. J. Brown, *Proc. Roy. Soc.,* **A226,** 531–542 (1954).
10. D. E. Bosley, *J. Appl. Polym. Sci.,* **8,** 1521–1529 (1964).
11. L. E. Alexander, *X-Ray Diffraction Methods in Polymer Science,* Wiley, New York, 1969.
12. H. M. Heuvel, R. Huisman, and K. C. J. B. Lind, *J. Polym. Sci. Polym. Phys. Ed.,* **14,** 921–940 (1976).
13. H. M. Heuvel and R. Huisman, *J. Appl. Polym. Sci.,* **22,** 2229–2243 (1978).
14. J. H. Dumbleton and B. B. Bowles, *J. Polym. Sci., A-2,* **4,** 951–958 (1966).
15. E. I. Du Pont De Nemours, USP 4,134,882 (16 January 1979).
16. J. D. Ferry, *Viscoelastic Properties of Polymers,* 2nd ed., Wiley, New York, 1970.
17. K. Kamide, T. Kuriki, and S. Manabe, *Polym. J.,* **18**(2), 167–171 (1986).
18. Mitsubishi Chem. Ind., JTN, 67-70 February 1980.
19. M. Kamezawa, K. Yamada, and M. Takayanagi, *J. Appl. Polym. Sci.,* **24,** 1227–1236 (1979).
20. I. Sakurada and K. Kaji, *J. Polym. Sci., Part C,* **31,** 57–76 (1970).
21. T. Thistlethwaite, R. Jakeways, and I. M. Ward, *Polymer,* **29**(1), 61–69 (1988).
22. C. L. Choy, M. Ito, and R. S. Porter, *J. Polym. Sci. Polym. Phys. Ed.,* **21,** 1427–1438 (1983).
23. T. Murayama, *Dynamic Mechanical Analysis of Polymeric Material,* Elsevier, New York, 1978.
24. G. Vassilatos, B. H. Knox, and H. R. E. Frankfort, in A. Ziabicki and H. Kawai, Eds., *High Speed Fiber Spinning,* Wiley, New York, 1985, Chapter 14.
25. R. S. Stein and F. H. Norris, *J. Polym. Sci.,* **21,** 381–396 (1956).
26. J. H. Dumbleton, *J. Polym. Sci., A-2,* **6,** 795–800 (1968).
27. J. Shimizu, N. Okui, and T. Kikutani, in A. Ziabicki and Kawai, Eds., *High Speed Fiber Spinning,* Wiley, New York, 1985, Chapter 15.
28. G. Perez, in A. Ziabicki and H. Kawai, Eds., *High Speed Fiber Spinning,* Wiley, New York, 1985, Chapter 12.
29. A. Ziabicki and L. Jarecki, in A. Ziabicki and H. Kawai, Eds., *High Speed Fiber Spinning,* Wiley, New York, 1985, Chapter 9.
30. A. Ziabicki, in A. Ziabicki and H. Kawai, *High Speed Fiber Spinning,* Wiley, New York, 1985, Chapter 2.
31. H. Yasuda, in A. Ziabicki and H. Kawai, Eds., *High Speed Fiber Spinning,* Wiley, New York, 1985, Chapter 13.
32. K. Fujimoto, K. Iohara, S. Owaki, and Y. Murase, *Sen-i Gakkaishi,* **44**(10), 477–482 (1988).
33. G. Y. Chen, Ph.D. Thesis, Fiber and Polymer Science Program, North Carolina State University, Raleigh, 1990.
34. H. M. Heuvel and R. Huisman, in A. Ziabicki and H. Kawai, Eds., *High Speed Fiber Spinning,* Wiley, New York, 1985, Chapter 11.
35. K. Fujimoto, K. Iohara, S. Owaki, and Y. Murase, *Sen-i Gakkaishi,* **44**(4), 171–176 (1988).
36. A. Jeziorny, *Acta Polym.,* **37**(4), 237–240 (1986).
37. C. P. Buckley, D. R. Salem, *Polymer,* **28**(1), 69–85 (1987).
38. K. Pournoor, J. C. Seferis, and G. Vassilatos, ANTEC Proc. 44th Annual Technical Conference, 1986, pp. 428–433.
39. K. Kamide, S. Manabe, and T. Kuriki, *Polym. J.,* **18**(2), 173–176 (1986).
40. S. Manabe and K. Kamide, *Polym. J.,* **16**(5), 375–389 (1984).
41. R. Huisman and H. M. Heuvel, *J. Appl. Polym. Sci.,* **37,** 595–616 (1989).
42. R. A. F. Moore and H. D. Weigmann, Book of Papers, 1985 International Conference and Exhibition AATCC, pp. 59–66.

Received October 29, 1991
Accepted November 4, 1991